Large Strain Torsion of Axially-Constrained Solid Rubber Bars

Wu, P.D.; Neale, K.W.; Giessen, E. van der

Published in:
Acta Mechanica Sinica

DOI:
10.1007/BF02486584

Publication date:
1994

ACTA MECHANICA SINICA, Vol.10, No.2, May 1994 ISSN 0567-7718
Science Press, Beijing, China
Allerton Press, INC., New York, U.S.A.

LARGE STRAIN TORSION OF AXIALLY-CONSTRAINED SOLID RUBBER BARS

P.D. Wu K.W. Neale+ E. Van der Giessen
(Laboratory for Engineering Mechanics, Faculty of Mechanical Engineering and Marine Technology, Delft University of Technology, The Netherlands)
+*(On leave from Université de Sherbrooke, Sherbrooke, Québec, Canada)*

ABSTRACT: Large strain fixed-end torsion of circular solid rubber bars is studied semi-analytically. The analyses are based on various non-Gaussian network models for rubber elasticity, some of which were proposed very recently. Results are presented in terms of predicted torque vs. twist curves and axial force vs. twist curves. In some cases, the predicted stress distributions are also given. The sensitivity of the second-order axial force to the employed models is considered. The predicted results are compared with experimental results found in the literature.

KEY WORDS: rubber, network model, large strain torsion

I. INTRODUCTION

The analysis of simple shear deformations has become a popular benchmark for testing the appropriateness of large strain constitutive models. In principle, simple shear can be produced approximately by torsion of thin-walled tubes with ends prevented from displacing in the axial direction. In fact, many experimental procedures based on torsion have used thin-walled specimens for which the state of the deformation has been assumed to be completely uniform[1]. Unfortunately, in order to avoid buckling in a finite deformation torsion experiment on a hollow tube, it is necessary that the thickness of the tube be at least 10–15% of the mean radius[2]. These tubes cannot really be considered to be thin and the deformation is not really homogeneous[3]. In addition to this, a thin hollow tube is much more difficult to manufacture and grip than a solid bar. Therefore in view of the various experimental problems, thin-walled tubes seem to be of less practical importance at large strains.

The torsion test of a solid cylindrical bar seems to be ideally suited for the experimental determination of material parameters in the range of large strains. The major advantage of this test over tensile tests is that deformations during torsion remain homogeneous in the axial direction until fracture. A second point of interest in large strain torsion relates to attempts to incorporate deformation-induced anisotropy into large strain constitutive models. Poynting[4] studied elastic torsion of solid wires with fixed ends (with axial constraint) and free ends (without axial constraint). From his experiments, Poynting pointed out that axial elongation occurs under free-end torsion, while axial compressive forces are created under fixed-end torsion. The prediction of similar second-order axial effects in large-strain

Received 14 January 1994

elastoplastic torsion of metals depends strongly on the constitutive model—in particular the description of anisotropic hardening[5,6,7]. Thus, the torsion test seems to provide a simple yet effective means for assessing the adequacy of the constitutive models.

The development of axial force has also been found in large strain fixed-end torsion of rubbers[8]. In the past, the analyses of large strain torsion of rubber seem to have been based exclusively on phenomenological constitutive models for rubber elasticity[9,10]. Phenomenological models have the distinct advantage of being relatively easy to implement in numerical analyses of large strain problems. However, they bear no relationship to the actual deformation mechanisms on the macromolecular level. For this purpose, non-Gaussian network models for rubber elasticity are required.

The development of macromolecular network models for rubber elasticity dates back to as early as the 1940s. These network theories are based upon the concept of a network of chains of randomly oriented rigid links that are connected at junction points which in rubber-like materials are provided by the chemical cross-links between macromolecules. Furthermore, these network theories use a so-called affine deformation scheme and assume that intermolecular interactions are negligible in comparison to intramolecular effects. The overall properties of the network are then obtainable by simply summing the contributions of the individual chains. Furthermore, the exact non-Gaussian treatment of a single chain is available (developed originally by Kuhn and Grun[11], James and Guth[12]). However, an exact treatment of the transition from an individual chain to network behaviour is very difficult owing to its mathematical complexity. In principle, this transition (through an averaging process) needs the orientations of the individual chains of the network, which was not available for arbitrary 3-D deformations until very recently[13].

Various simplified averaging procedures for obtaining the network response have been proposed[13]. Among these simplified models, the so-called three-chain model assumes that a network containing n chains per unit volume is equivalent to three independent sets of $n/3$ single chains in three orthogonal directions. Thus, the actual spatial distribution of chains is sampled in three orthogonal orientations. Very recently, Arruda and Boyce[14,15] proposed a so-called eight-chain model to sample eight spatial chain orientations. Obviously, these models are approximate representations of the actual spatial distribution of molecular chains. They can be regarded to sample a set of particular directions among all possible orientations. More precisely, the three-chain model would overestimate the contribution of the chain collection oriented along the direction of major principal extension, while the eight-chain model would underestimate the stiffness of the network[16].

The full network formulation by Wu and Van der Giessen[13,17,18] accounts accurately for the actual spatial orientation distribution of molecular chains. Treloar and Riding[19] had already developed a rubber elasticity theory based on such a full network description, but their considerations were limited to deformations with biaxial extension along fixed axes under plane stress conditions. Our model extends their theory to a general formulation valid for 3-D deformation processes. Furthermore, our model allows us to avoid calculating principal stretches and principal directions of deformation[18]. The modelling centres around a general treatment of the orientation distribution of molecular chains and their evolution as deformation progresses. This description utilizes the idea of Chain Orientation Distribution Function (CODF), which is governed by balance equations that express physically well-understood conservation features. Assuming the network to deform affinely with the

deformation of the continuum it is embedded in, a closed-form solutions have been derived for this CODF, which thus contain the complete information of the orientation distribution of molecular chains at any stage of the deformation. This solution is then used to develop the rubber elasticity model by averaging out the contribution to the network response of individual chains over all chain orientations. The full network model has been found to be able to pick up many aspects of the mechanical behaviour of rubbers at various different large deformations[13,18,20].

However, the application of the rubber network models has so far been restricted to uniform deformations. Obviously, the torsion test on a solid circular bar involves stress and deformation gradients along the radius of the bar, as well as non-proportional stressing histories and rotations of the principal axes of strain for each element of the cross-section. Therefore, the analysis of large strain solid bar torsion is considerably more involved. Fortunately, Neale and Shrivastava[5] have found that if the behaviour is axisymmetric, axially homogeneous and incompressible, semi-analytical solutions can be obtained for solid bars subjected to fixed-end torsion. In this paper, we study large strain fixed-end torsion of rubbers using that method[5]. Results are presented in terms of predicted torque vs. twist curves and axial force vs. twist curves. In some cases, the predicted stress distributions are also given. The predicted results are compared with experimental results for a vulcanized rubber given by Rivlin and Saunders[8].

Tensors will be denoted by bold-face letters. The tensor product is denoted by $\otimes$ and the following operation for second-order tensor applies ($\boldsymbol{a} = a_{ij}\boldsymbol{e}_i \otimes \boldsymbol{e}_j$, $\boldsymbol{b} = b_{ij}\boldsymbol{e}_i \otimes \boldsymbol{e}_j$, $\boldsymbol{e}_i$ being a Cartesian basis): $\boldsymbol{ab} = a_{ik}b_{kj}\boldsymbol{e}_i \otimes \boldsymbol{e}_j$. Superscripts T and -1 denote the transverse and inverse of a second-order tensors, respectively. The trace is denoted by tr.

II. NETWORK MODELS FOR RUBBER ELASTICITY

1. Full Network Model

Wu and Van der Giessen[13,18] introduced a so-called molecular Chain Orientation Distribution Function (CODF), denoted by $C(\Theta, \Phi; t)$, such that the relative density of molecular chains, at some instant t, whose end-to-end vector $\boldsymbol{r}$ has an orientation in the range between (Θ, Φ) and $(\Theta + \mathrm{d}\Theta, \Phi + \mathrm{d}\Phi)$ is given by $C(\Theta, \Phi; t)\sin\Theta\mathrm{d}\Theta\mathrm{d}\Phi$. Note that $\sin\Theta\mathrm{d}\Theta\mathrm{d}\Phi$ is the area on a unit sphere spanned by the interval $(\mathrm{d}\Theta, \mathrm{d}\Phi)$ and that t is just a time-like monotonic parameter. With n denoting the number of chains per unit volume, the actual number of chains between (Θ, Φ) and $(\Theta + \mathrm{d}\Theta, \Phi + \mathrm{d}\Phi)$ then is

$$\mathrm{d}n = nC(\Theta, \Phi; t)\sin\Theta\mathrm{d}\Theta\mathrm{d}\Phi \tag{1}$$

For a virgin, unstrained material the orientation of network chains can usually be considered to be distributed in a random fashion; then C will be independent of Θ and Φ, and the material's response is instantaneously isotropic. When the material is deformed, all chains are stretched and, at the same time, rotated. Hence, the CODF will develop into a nonuniform distribution that can be quite severe as has been demonstrated in Wu and Van der Giessen[13]. Thus, texture development in the sense of molecular chain distributions is described in this model in terms of this CODF.

Assuming the network to deform affinely with some three-dimensional deformation process represented by the deformation gradient tensor $\boldsymbol{F}$ of the continuum it is embedded in, each chain's end-to-end vector $\boldsymbol{r}_0$ in the initial state is taken to be strained and rotated

to the vector $\boldsymbol{r}$ in the current state in an affine manner, i.e. $\boldsymbol{r} = \boldsymbol{F}\boldsymbol{r}_0$. Since we assume the network to be incompressible, the deformation gradient tensor satisfies det $\boldsymbol{F}$=1. It can be shown[13,18] that in an arbitrary state of deformaiton, the CODF for an initially random network can be expressed as follows

$$C = C_0\lambda_c^3(\Theta, \Phi; \boldsymbol{F}) \tag{2}$$

where $C_0 = 1/4\pi$ is the initial uniform distribution, and where λ_c is the chain stretch which can be obtained from $\boldsymbol{F}$ by

$$\lambda_c^{-2} = \boldsymbol{m}(\boldsymbol{F}\boldsymbol{F}^{\mathrm{T}})^{-1}\boldsymbol{m} \tag{3}$$

Here, $\boldsymbol{m}$ is the unit vector $\boldsymbol{m} = \boldsymbol{r}/r = m_i\boldsymbol{e}_i(r = ||\boldsymbol{r}||)$ along the end-to-end vector $\boldsymbol{r}$, in the current deformed state with components

$$m_1 = \sin\Theta\cos\Phi \qquad m_2 = \sin\Theta\sin\Phi \qquad m_3 = \cos\Theta \tag{4}$$

Here, we have substituted the deformation gradient tensor as the time-like parameter t in the previous expressions for the CODF. This is possible since, as a consequence of the affine deformation assumption, the distortion of the network is independent of the rate of deformation, so that t only needs to be some monotonic parameter. Identifying t with $\boldsymbol{F}$ will turn out to be convenient for further development. For a detailed derivation of (2) we refer to Wu and Van der Giessen[13,18].

Consider a single chain between two junction points, with its end-to-end vector $\boldsymbol{r}$ in the current state being specified by angular coordinates Θ and Φ with respect to some fixed frame of reference defined by the set of orthonormal base vectors $\boldsymbol{e}_i$ (see Fig.1). We further assume that this single chain has a given stretch λ_c in current state. If the chain contains N links of length l, the length of the unstrained free chain r_0 is given by the root-mean-square value $\sqrt{N}l$. By considering the statistical distribution of possible link angles at a given stretch λ_c, Kuhn and Grun[11] were the first to derive the well-known non-Gaussian relationship between force f_c and stretch λ_c for the stretched chain, which could be transformed into a relationship between the Cauchy stress σ_c acted on the continuum in which the chain is embedded and the stretch in the form[18]

$$\sigma_c = C^R\sqrt{N}\lambda_c\mathcal{L}^{-1}\Big(\frac{\lambda_c}{\sqrt{N}}\Big) \tag{5}$$

where C^R is known as the rubbery modulus and $\mathcal{L}$ is the Langevin function defined by $\mathcal{L}(\beta) = \coth\beta - 1/\beta$.

Wu and Van der Giessen[18] further introduced a so-called micro-stress tensor $\boldsymbol{\sigma}_c$ by

$$\boldsymbol{\sigma}_c = \sigma_c(\boldsymbol{m}\otimes\boldsymbol{m}) - p\boldsymbol{I} \tag{6}$$

which can be interpreted as the contribution of the single chain to the stress of the network. The hydrostatic pressure p is included because of incompressibility. The hydrostatic pressure

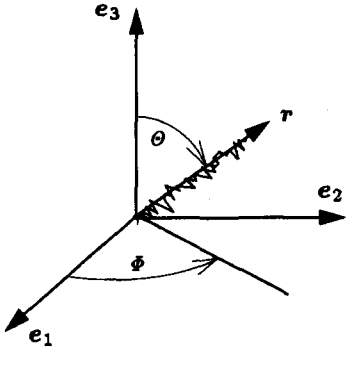

Fig.1 A single chain in strained state; definition of geometric quantities

p is included because of incompressibility. The overall or macrostress tensor $\boldsymbol{\sigma}$ of the network is then obtainable by simply averaging the micro-stress tensor $\boldsymbol{\sigma}_c$ of the individual chains, i.e.

$$\boldsymbol{\sigma} = \frac{1}{n}\int \boldsymbol{\sigma}_c \mathrm{d}n \tag{7}$$

With dn being given by (1) and the CODF by (2), we finally obtain from (7) with the help of (5) and (6) for the Cartesian stress components, $\boldsymbol{\sigma} = \sigma_{ij}\boldsymbol{e}_i \otimes \boldsymbol{e}_j$

$$\sigma_{ij} = \frac{1}{4\pi} C^R \sqrt{N} \int_0^{\pi} \int_0^{2\pi} \lambda_c^4 \mathcal{L}^{-1}\Big(\frac{\lambda_c}{\sqrt{N}}\Big) m_i m_j \sin\Theta \mathrm{d}\Theta \mathrm{d}\Phi - p\delta_{ij} \tag{8}$$

with λ_c determined from (3) as a function of the deformation gradient tensor $\boldsymbol{F}$ and the orientation (Θ, Φ). The hydrostatic pressure p is left unspecified by the constitutive equations and is to be determined from the boundary conditions.

2. Simplified Models

Now consider two simplified network models that have been proposed in the literature, namely the three-chain model and the eight-chain model. The three-chain model assumes that a network containing n chains per unit volume is equivalent to three independent sets of $n/3$ chains per unit volume parallel to the Eulerian principal axes $\boldsymbol{e}_i^E$ as shown in Fig.2(a). The principal values of the stress tensor according to this model are given in terms of the principal stretches λ_i by[21]

$$\sigma_i^{3-\mathrm{ch}} = \frac{C^R\sqrt{N}}{3}\lambda_i \mathcal{L}^{-1}\Big(\frac{\lambda_i}{\sqrt{N}}\Big) - p \qquad (\text{no sum}) \tag{9}$$

Once these principal stresses are evaluated, the Cauchy stress tensor $\boldsymbol{\sigma}^{3-\mathrm{ch}}$, whose principal axes concide with the Eulerian triad $\boldsymbol{e}_i^E$, is constructed by

$$\boldsymbol{\sigma}^{3-\mathrm{ch}} = \sum_{i=1}^{3} \sigma_i^{3-\mathrm{ch}} (\boldsymbol{e}_i^E \times \boldsymbol{e}_i^E)$$

The eight-chain model for rubber elasticity was proposed by Arruda and Boyce[14,15] and considers a set of eight chains connecting the central junction point and each of eight corners of the unit cube as shown in Fig.2(b). The stress tensor according to the eight-chain model, $\boldsymbol{\sigma}^{8-\mathrm{ch}}$, is found as

$$\boldsymbol{\sigma}^{8-\mathrm{ch}} = \frac{C^R\sqrt{N}}{3\lambda_c}\mathcal{L}^{-1}\Big(\frac{\lambda_c}{\sqrt{N}}\Big)\boldsymbol{F}\boldsymbol{F}^{\mathrm{T}} - p\boldsymbol{I} \tag{10}$$

with

$$\lambda_c = \sqrt{\frac{1}{3}\mathrm{tr}(\boldsymbol{F}\boldsymbol{F}^{\mathrm{T}})}$$

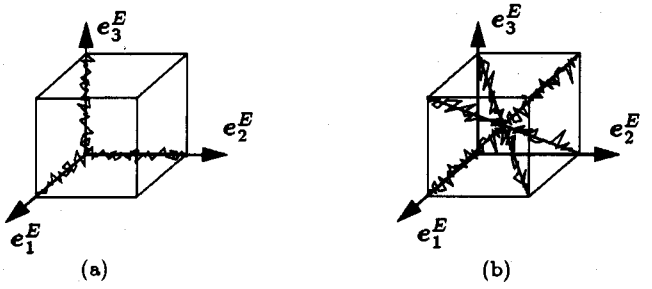

Fig.2 Schematic representation of the three-chain model (a) and the eight-chain model (b)

Comparing these three-chain and eight-chain samplings with the actual three-dimensional initial random distribution of molecular chains, the three-chain model would overestimate the actual stiffness of the network, while the eight-chain model would probably give a lower bound. Indeed, the stress response predicted by our full network model (8) is, for the same values of N and n, always in between that predicted by the three-chain model and eight-chain model, respectively[13,18]. However, the integrations involved in (8) require a rather time-consuming numerical procedure. An approximation of the full integration has been found[17] in the form of combination of the three-chain and eight-chain models through

$$\boldsymbol{\sigma} = (1-\rho)\boldsymbol{\sigma}^{3-\mathrm{ch}} + \rho\boldsymbol{\sigma}^{8-\mathrm{ch}} \tag{11}$$

where the parameter ρ may be a constant or related to some other physical quantity which is, for instance, related to the maximal principal stretch $\lambda_{\max} = \max(\lambda_1, \lambda_2, \lambda_3)$ via

$$\rho = 0.85\frac{\lambda_{\max}}{\sqrt{N}} \tag{12}$$

where the factor 0.85 was chosen to give the best correlation with full integrations of (8). In this way, the eight-chain contribution in (10) becomes increasingly important when $\lambda_{\max}$ approaches the limit stretch $\sqrt{N}$.

III. PROBLEM FORMULATION AND METHOD OF SOLUTION

We consider a homogeneous, incompressible solid circular bar of radius R and length L subjected to a twist φ (see Fig.3). The lateral surface of the bar is stress-free and all properties are assumed to be axisymmetric and homogeneous along the axial direction. Although anisotropy will be induced during the deformation process, the behaviour remains axisymmetric and the bar remains circular cylindrical. The end faces of the bar are constrained to the extent that they remain plane and perpendicular to the axial direction, so that we may assume that any cross-section of the bar remains plane. For the fixed-end condition considered here, the end faces of the bar are fully constrained axially so that there is no axial displacement, thus allowing for the development of an axial force F.

The kinematics of the problem is readily established with the aid of a spatially fixed cylindrical coordinate system $x^i = (\theta, z, r)$ with associated orthonormal base vectors $\boldsymbol{e}_1 = \boldsymbol{e}_\theta$, $\boldsymbol{e}_2 = \boldsymbol{e}_z$, $\boldsymbol{e}_3 = \boldsymbol{e}_r$. These base vectors are associated with material elements in their current, deformed state, so that tensor components with respect to this basis represent

physical components. The deformations are assumed such that if the initial coordinates of a material point are (θ_0, z, r), its current coordinates are given by (θ, z, r), with $\theta = \theta_0 + (\varphi/L)z$. Accordingly, the components L_{ij} of the velocity gradient tensor $\boldsymbol{L} = L_{ij}\boldsymbol{e}_i \otimes \boldsymbol{e}_j$ are such that

$$[L_{ij}] = \begin{bmatrix} 0 & \dot{\gamma} & 0 \\ 0 & 0 & 0 \\ 0 & 0 & 0 \end{bmatrix} \tag{13}$$

where $\dot{\gamma} = r(\dot{\varphi}/L)$. Thus, each element of the bar is in a state of simple shear in the θ-z plane, where the shear strain γ is directly proportional to the radial distance r. That is

$$\gamma(r) = \frac{r}{R}\Gamma \tag{14}$$

where $\Gamma = (R/L)\varphi$ represents the shear strain at the outer surface of the bar.

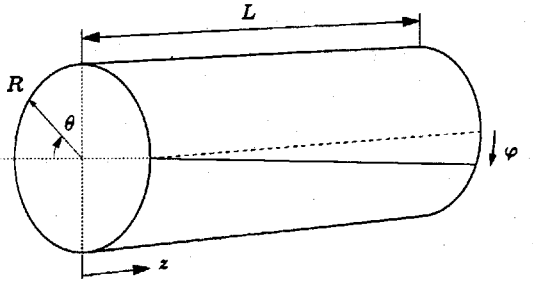

Fig.3 Schematic representation of an axially-constrained solid circular bar under torsion

Neale and Shrivastava[5] have found that if the behaviour is axisymmetric, axially homogeneous and incompressible, semi-analytical solutions can be obtained for solid bars subjected to fixed-end torsion. This is possible since each material point is in this case simply loaded in simple shear under an additional hydrostatic pressure, where the shear γ is directly proportional to the radius r, as shown in (13) and (14). To apply this semi-analytical method, we require the values of the deviatoric stress components s_{ij} during simple shear as a function of the shear deformation γ, which is then readily translated into the stress deviator distribution $s_{ij}(r)$. To obtain the actual stress distribution $\sigma_{ij} = s_{ij} - p\delta_{ij}$ (where δ_{ij} is Kronecker delta), the hydrostatic pressure distribution $p(r)$ is needed[5].

For the above conditions, the only equation of equilibrium which is not identically satisfied is the relation

$$r\frac{\mathrm{d}\sigma_{rr}}{\mathrm{d}r} + \sigma_{rr} - \sigma_{\theta\theta} = 0$$

This can be written in terms of p and the known $s_{ij}(r)$ distribution as follows

$$\frac{\mathrm{d}p}{\mathrm{d}r} = \frac{\mathrm{d}s_{rr}}{\mathrm{d}r} + \frac{1}{r}(s_{rr} - s_{\theta\theta}) \tag{15}$$

Integrating the resulting equation and using the boundary condition $\sigma_{rr}(R) = 0$, gives the hydrostatic pressure distribution

$$p(r) = s_{rr} - \int_r^R \frac{1}{r}(s_{rr} - s_{\theta\theta})\mathrm{d}r \tag{16}$$

Combining this with the stress deviator distribution gives $\sigma_{ij}(r)$. The resultant torque M and axial force F are computed by

$$M(\Gamma) = 2\pi \int_0^R r^2 \sigma_{\theta z} \mathrm{d}r \tag{17}$$

and

$$F(\Gamma) = 2\pi \int_0^R r \sigma_{zz} \mathrm{d}r \tag{18}$$

respectively. Since $\sigma_{\theta z} = s_{\theta z}$ the hydrostatic pressure has no influence on M.

IV. RESULTS

The torsion problem described in Section III involves a number of nondimensional groups, among which are the following

$$\Gamma = \frac{R}{L}\varphi \qquad \tau = \frac{2M}{\pi R^3 C^R} \qquad \sigma = \frac{F}{\pi R^2 C^R} \tag{19}$$

These quantities can be used to present the overall response of a specimen under fixed-end torsion, irrespective of the actual dimensions of the specimen. Note that the normalized torque parameter τ in (19) differs from that in Van der Giessen et al.[7], for reason to become clear shortly.

Figure 4 shows the predicted normalized torque responses according to various network models. The value of the network parameter $N = 25$ was used for all three models; it was simply selected as representative value of N. What this result clearly shows is that relative to the full network model, the three-chain approximation tends to overestimate the stiffness at large twists, while the eight-chain model tends to underestimate this. It is clear that all models give virtually identical predictions for small shear strains up to $\Gamma \approx 1.8$. It is only for large strains that considerable differences arise. Furthermore, the approximation (11) for the full network response in terms of τ is seen to be very accurate up to very large twists. Comparing Fig.4 with the uniform simple shear results reported by Wu and Van der Giessen[17], it is found that the overall trends obtained for the normalized torque of the solid bar in fixed-end torsion seems to be similar to the shear stress response in simple shear.

The predicted normalized axial forces are presented in Fig.5. The prime characteristic of the response is that the axial force developed during twisting is compressive. All three network models give virtually identical predictions up to $\Gamma \approx 2.3$. For large values of twist, the three-chain model predicts very large compressive forces, which are associated with the stretching of the network affinely with the deformation. Initially, the principal stretch directions are oriented at 45° relative to the $\boldsymbol{e}_\theta$-$\boldsymbol{e}_z$ axes, and this orientation slowly rotates towards the final ideal $\boldsymbol{e}_\theta$-$\boldsymbol{e}_z$ directions with ongoing shearing. The limit stretch of the network is attained long before such final orientations are reached, thus explaining the very substantial axial force. When using the eight-chain model, we see that the magnitude of the axial force reduces drastically. Again, the predicted axial force by the full network model is between that predicted by the three-chain model and the eight-chain model respectively. Furthermore, the overall qualitative trends obtained for the axial force of the fixed-end solid bar torsion are similar to the evolution of the normal stress in simple shear, as reported by Wu and Van der Giessen[17]. Again we see that the approximation (11) for the full

network response in terms of σ is very accurate up to very large twists. In the remainder of this Section, all results according to the full network model have been obtained with the approximation (11).

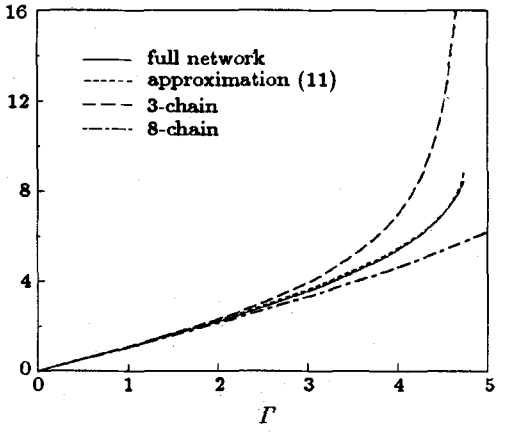

Fig.4 Predicted torque for fixed-end torsion according to different network models with $N = 25$

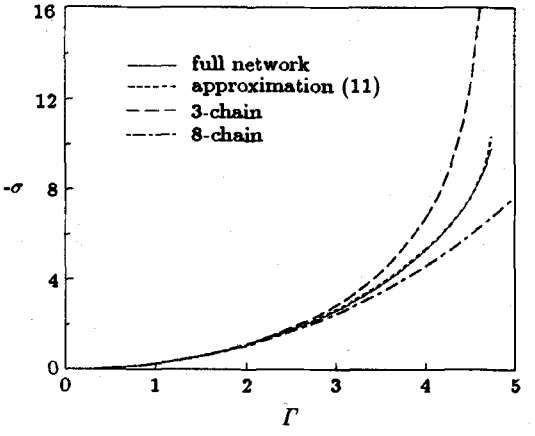

Fig.5 Predicted axial force for fixed-end torsion according to different network models with $N = 25$

Figure 6 shows the stress distributions, according to the full network model, across the bar when (a) $\Gamma = 0.6$ and (b) $\Gamma = 4.7$. It is found that the stresses in the bar are highly nonuniform. The reason is that the material close to the axis of the solid bar remains in the small deformation state up to the moment that the maximum stretch at the outer surface of the bar approaches the limit stretch $\sqrt{N}$ of the network. For practical purposes, it may be of interest however to have an approximate tool to link the twisting of a solid bar to homogeneous simple shear. If the shear stress distribution is approximated to be linear over the entire cross-section, the shear stress at the outer surface of the bar τ is readily found to be related to the applied torque M through the quantity τC^R defined in (19). To assess the accuracy of this approximation, we plot in Fig.7 the torque responses found for the solid bar in comparison with the shear stress σ_{12} for homogeneous simple shear to a shear strain Γ obtained by direct straightforward integration of the constitutive equations. It is seen that the simple representation in terms of τ gives a reasonable estimate of the simple shear behaviour up to strains $\Gamma \approx 2.2$ (see Fig.7). At larger strains, the linear shear stress distribution assumption is no longer valid due to the very strongle non-Gaussian effect and the simple representation in terms of τ (19) cannot give an adequate agreement with homogeneous simple shear.

To enable a direct comparison with experimental data for vulcanized rubber reported by Rivlin and Saunders[8] we have taken the actual dimensions to be the same as in Rivlin and Saunders[8], i.e. $R = 1.27$ cm and $L = 2.54$ cm. Obviously, the values of the material parameters N and C^R have to be determined for a quantitative prediction. As pointed out by Wu and Van der Giessen[13], the full network model as well as the simplified three-chain model and eight-chain model are able to reproduce experimental rubber stress-strain data for a certain deformation and material by selecting the material parameters N and C^R for the given model. A more important aspect appears to be the description of the network

response under different states of deformation. For that purpose, we take the following procedure[13,15]. The network parameters N and C^R are fitted for equi-biaxial stretch data, and then used to predict fixed-end torsion. The equi-biaxial stretching is characterized by the principal stretches $\lambda_1 = \lambda_2 = \lambda, \lambda_3 = \lambda^{-2}$ along fixed directions, while the material is in a state of plane stress, i.e. $\sigma_{33} = 0$. Figure 8 shows the true stress (σ_{11}) response in the stretching direction, where the values of $N = 50$ and $C^R = 0.36$ MPa were found to give the best correlation with the equi-biaxial tension data[8].

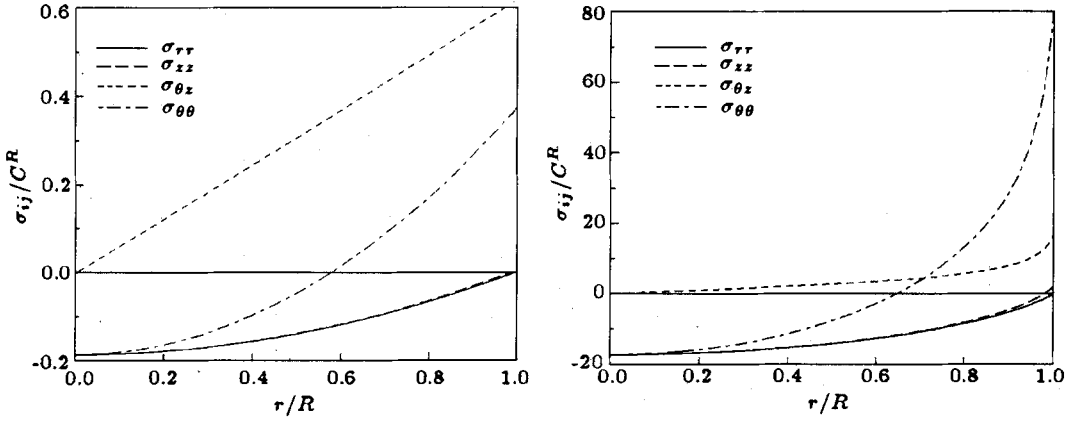

Fig.6 Predicted stress distributions across the bar, according to the full network model with $N = 25$, for (a) $\Gamma = 0.6$ and (b) $\Gamma = 4.7$

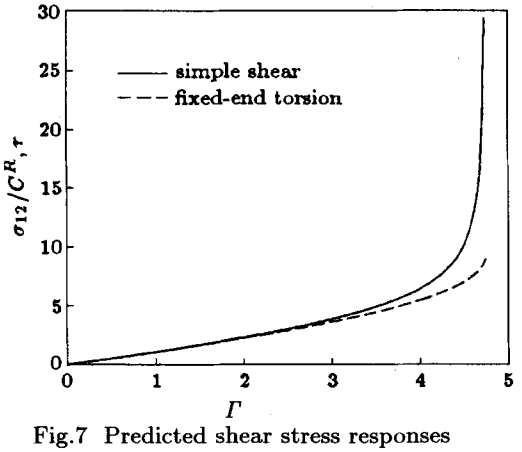

Fig.7 Predicted shear stress responses in simple shear and torsion for the full network model with $N = 25$

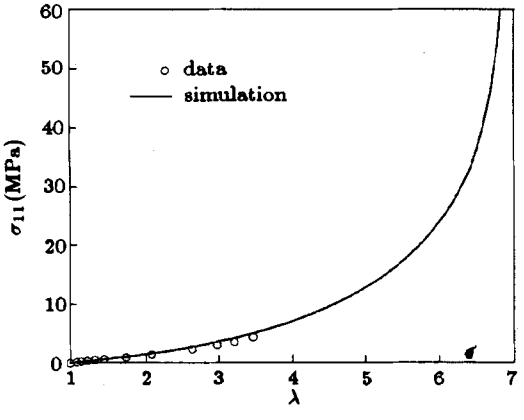

Fig.8 Predicted true stress vs. stretch for equi-biaxial tension of a vulcanized rubber according to the full network model with N=50 and C^R=0.36MPa. The experimental data is taken from [8]

The predicted results of fixed-end torsion using these values of the parameters are given in Figs.9 and 10. It is found that the predicted torque response is in a good agreement with the experimental results (Fig.9). However, the predicted axial forces are systematically lower in magnitude than the experimental measurements, although the overall trends of their evolutions are

quite similar (Fig.10). It is noted however that the value of the experimentally measured axial force corresponding to $\Gamma = 0$ is not zero. That would, in general, be the case only if the material are anisotropic in the undeformed state. The initial anisotropy could be a result of the manufacturing process.

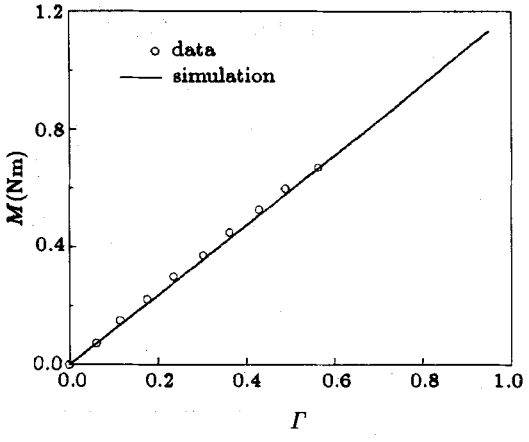

Fig.9 Predicted torque for fixed-end torsion of a vulcanized rubber according to the full network model with $N = 50$ and C^R=0.36MPa. The experimental data is taken from [8]

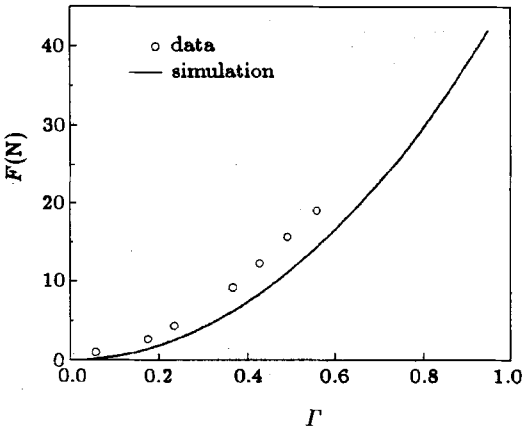

Fig.10 Predicted axial force for fixed-end torsion of a vulcanized rubber according to the full network model with $N = 50$ and C^R=0.36MPa. The experimental data is taken from [8]

V. DISCUSSION AND CONCLUSION

In this paper, we have analyzed the large-strain elastic torsion of axially constrained circular cylindrical bars of rubbers, based on the network models for rubber elasticity, using a semi-analytical method proposed by Neale and Shrivastava[5].

Because of the stress and deformation gradients created in the solid bar and the development of hydrostatic pressure, the predicted responses for the torsion problem differ considerably from those for uniform simple shear. As expected, the stress distributions in the solid bar are quite nonuniform (see Fig.6). The reason for this is that the material close to the axis of the bar remains in the small deformation state up to the moment that the maximum stretch at the outer surface of the bar approaches the limit stretch $\sqrt{N}$ of the network.

The compressive axial force induced in torsion is mainly due to the development and subsequent rotation of the induced anisotropy. For the rubbers considered here, the anisotropy is associated with the stretching of the cross-linked molecular chain structure. It is found that all three network models for rubber elasticity discussed in Section II give virtually identical predictions for shear strains up to $\Gamma \approx 2$. For larger twists, the three-chain model predicts very large compressive forces, but when using the eight-chain model, we see that the magnitude of the axial force reduces drastically (see Fig.5). The predicted axial force based on the full network model is in between that predicted by the three-chain model and the eight-chain model respectively. Furthermore, the sensitivity of this second-order axial

force to the adopted constitutive models for rubbers considered here is much less pronounced than that for metals[7]. Nevertheless, the predictions of the second-order optical properties in simple shear depend strongly on the network models for rubber photoelasticity[18].

The approximation (11) to the full network model in terms of the three-chain and eight-chain representations is found to be very accurate up to very large twists not only for the shear stress but also for the normal stress. Based on this observation and the numerical tests on different types of deformation and rubbers[13,18], we conclude here that this particular approximation to the full network model is a very accurate tool for different types of deformation over the entire range of strains. Since the full network model involves rather time-consuming integrations, the approximation turns out to be very useful when one wishes to incorporate the model in finite element computations.

The predicted response of a specimen according to the full network model has been compared with available experimental data for a vulcanized rubber, based on material properties determined from an equi-biaxial tension test for the same rubber. Generally, the agreement is reasonable. Since equi-biaxial tension and torsion are rather different deformation processes, the torsion analysis further supports our conclusion[13,18]; namely, that the full network model for rubber elasticity does pick up the dependence of the state of deformation observed experimentally in rubber materials.

Perhaps, the most important difference between the simulated and experimental response to torsion is that our simulation tends to underestimate the second-order axial effect. However, it is important to note that the value of the experimentally measured axial force corresponding to $\Gamma = 0$ is not zero. In general, that would be the case only if the material are anisotropic in the undeformed state. Such initial anisotropy could be induced during the manufacturing processes. If the specimen used in torsion test is initially isotropic, a much better agreement between experimental results and the predictions would be expected.

With regard to the constitutive models, we have noted that there are several assumptions that underlie the present network concept, and which can act as potential sources of discrepancy with experiments. First of all, the affine deformation assumption is known to hold with high accuracy at low deformations, but it has been suggested that as the deformation increases, the behaviour of a real network approaches the so-called phantom network in which the junction points move independently of the continuum[22]. Secondly, we assumed that the junction points in the network provide permanent nodes in the network; however, it has been suggested that the molecular chains may also slide relative to each other at so-called sliplinks[23]. Finally, intermolecular effects are neglected in the present network models. However, when chains are rotated towards a common axis to such an extent that they become aligned up at very large deformations, intermolecular interactions are no longer negligible. Molecular dynamics simulations[24] seem to indicate that this may be a significant effect already at relatively small deformations in the Gaussian regime, and it may be expected to be ever more important at the large strain level. All these constitutive aspects require further study both theoretically and experimentally.

A final related point is that torsion with the ends free to displace axially, may perhaps be even more convenient from an experimental point of view. Of particular importance is the development of significant axial strains during free-end torsion, and that the prediction of this so-called Poynting effect[4] shows a remarkably strong dependence on the constitutive models. However, the analysis of free-end torsion is significantly more involved. Obviously,

the present semi-analytical method is no longer valid for free-end torsion. Fortunately, Wu and Van der Giessen[3,6,25] have developed a numerical approach based on a simple but effective dedicated finite element, which is suited for the analysis of large-strain torsion of circular solid bars as well as thin-walled tubes under free-end conditions as well as fixed-end and intermediate conditions.

REFERENCES

[1] White CS, Bronkhorst CA and Anand L. An improved isotropic-kinematic hardening model for moderate deformation metal plasticity. *Mech Mater*, 1990, 10: 127–147

[2] Khen R and Rubin MB. Analytical modelling of second order effects in large deformation plasticity. *Int J Solids Structures*, 1992, 29: 2235–2258

[3] Wu PD and Van der Giessen E. On large strain inelastic torsion of glassy polymers. *Int J Mech Sci*, 1993, 35: 935–951

[4] Poynting JH. On pressure perpendicular to the shear planes in finite pure shears and on lengthening of loaded wires when twisted. *Proc R Soc Lond*, 1909, A82: 546–559

[5] Neale KW and Shrivastava SC.. Analytical solutions for circular bars subjected to large strain plastic torsion. *J Appl Mech* , 1990, 57: 293–306

[6] Wu PD and Van der Giessen E. Analysis of elastic-plastic torsion of circular bars at large strains. *Arch Appl Mech*, 1991, 61: 89–103

[7] Van der Giessen E, Wu PD and Neale KW. On the effect of plastic spin on large strain elastic-plastic torsion of solid bars. *Int J Plast*, 1992, 8: 773–801

[8] Rivlin RS and Saunders DW. Large elastic deformations of isotropic materials VII. Experiments on the deformation of rubber. *Phil Trans R Soc*, 1951, A243: 251–288

[9] Ogden RW, Chadwick P. On the deformation of solid and tubular cylinders of incompressible isotropic elastic material. *J Mech Phys Solids*, 1972, 20: 77–90

[10] Ogden RW, Chadwick P and Haddon EW. Combined axial and torsional shear of a tube of incompressible isotropic elastic material. *Quart Journ Mech and Applied Math*, 1973, XXVI: 23–41

[11] Kuhn W and Grun F. Beziehuugen zwischen elastischen konstanten uud dehuungsdoppelbrechung hochelastischer stoffe. *Kolloidzeitschrift*, 1942, 101: 248–271

[12] James HM and Guth E. Theory of the elastic properties of rubber. *J Chem Phys*, 1943, 11: 455–481

[13] Wu PD and Van der Giessen E. On improved network models for rubber elasticity and their applications to orientation hardening in glassy polymers. *J Mech Phys Solids*, 1993, 41: 427–456

[14] Arruda EM and Boyce MC. Evolution of plastic anisotropy in amorphous polymers during finite straining. In: Boehler J-P and Khan AS eds. Anistotropy and Localization of Plastic Deformation. London: Elsevier Applied Science, 1991. 483–488

[15] Arruda EM and Boyce MC. A three-dimensional constitutive model for large stretch behaviour of rubber materials. *J Mech Phys Solids*, 1993, 41: 389–412

[16] Dahoun A, G'Sell C, Molinari A and Canova GR. Plastic behaviour and deformation textures of poly (ether ether ketone) under uniaxial tension and simple shear. 1993 (submitted for publication, 1993)

[17] Wu PD and Van der Giessen E. On improved 3-D non-Gaussian network models for rubber elasticity. *Mech Res Comm*, 1992, 19: 427–433

[18] Wu PD and Van der Giessen E. On network descriptions of mechanical and optical properties of rubbers. (submitted for publication)

[19] Treloar LRG and Riding G. A non-Gaussian theory for rubber in biaxial strain. I. Mechanical properties. *ProcR Soc Lond*, 1979, A369: 261–280

[20] Dahoun A. Comportement Plastique et Textures de Deformation des Polymeres Semi-crystallins en Traction Uniaxiale et en Cisaillement Simple. Ph D Thesis. Institut National Polytechnique de Lorraine, Nancy, France, 1992

[21] Wang MC and Guth E. Statistical theory of networks of non-Gaussian flexible chains. *J Chem Phys*, 1952, 20: 1144–1157

[22] Mark JE and Erman B. Rubberlike Elasticity: A Molecular Primer. New York: Wiley, 1988

[23] Ball RC, Doi M, Edwards SF and Warner M. Elasticity of entangled network. *Polymer*, 1981, 22: 1010–1018

[24] Gao J and Weiner JH. Chain force concept in systems of interacting chains. *Macromolecules*, 1991, 24: 5179–5191

[25] Wu PD and Van der Giessen E. Large strain visco-plastic torsion of circular bars of glassy polymers. In: Lee WB ed. Advances in Engineering Plasticity and its Applications. Amsterdam: Elsevier Science Publishers BV, 1993. 477–484